J Wood Sci (2007) 53:47–53
DOI 10.1007/s10086-006-0822-3

ORIGINAL ARTICLE

Minoru Yada · Gyosuke Meshitsuka

Spectral analysis of the successive degradation process of kraft lignin by alkaline oxygen treatment

Received: December 12, 2005 / Accepted: May 10, 2006 / Published online: October 8, 2006

Abstract Softwood kraft lignin was subjected to alkaline oxygen treatment in a fundamental study of lignin degradation. Two different spectral changes were observed in the time course of ultraviolet-visible spectra along with the progress of the treatment. These spectral changes could be recognized as proceeding along certain temporal functions that were based on second-order decays with different half-lives. The spectral changes were defined as "fast change" and "slow change." The fitting studies on the amount of total protons on the unsaturated and aromatic systems, the amount of unconjugated phenolic substructure determined by differential ionization spectra, and the amount of methoxyl group with temporal functions showed that two reaction types (formation of muconate derivatives and *ortho*-quinone derivatives) can be expected as the major modification types occurring during fast change. The fitting study of the time course of infrared attenuated total reflectance (ATR) spectra gave corresponding infrared ATR spectral features of fast and slow changes. The occurrence of the formation of muconate derivatives by fast change was strongly supported by the spectral feature of fast change. On the other hand, it is suggested that the aromatic structure of lignin was further degraded during slow change. In addition, formation of resistant phenolic substructures is suggested as another possible modification type occurring by fast change.

Key words Kraft lignin · Oxygen delignification · Numerical analysis · Spectroscopy

M. Yada (✉) · G. Meshitsuka
Laboratory of Wood Chemistry, Department of Biomaterial Sciences, Graduate School of Agricultural and Life Sciences, The University of Tokyo, 1-1-1 Yayoi, Bunkyo-ku, Tokyo 113-8657, Japan
Tel. +81-35-841-5264; Fax +81-35-802-8862
e-mail: yadamistry@yahoo.co.jp

Parts of this article were presented at the 13th International Symposium on Wood, Fiber, and Pulping Chemistry, Auckland, New Zealand, May 2005

Introduction

In the process of the production of bleached kraft pulp, oxygen delignification under alkaline conditions is widely applied as the subsequent delignification process of kraft cooking. However it has been claimed that only 50% of residual lignin can be removed during oxygen delignification, because further oxygen treatment results in the degradation of carbohydrates.[1] This means that the remaining 50% of residual lignin needs to be removed or degraded by the use of other bleaching reagents like hydrogen peroxide and chlorine dioxide, which impose relatively high costs and environmental loads. Thus, further improvement of the reaction selectivity of oxygen delignification toward residual lignin is one of the key strategies for making the whole pulping process more economically and ecologically sustainable.

Mechanisms of delignification by oxygen have long been studied from the perspective of degradation mechanisms and kinetics using lignin model compounds.[2,3] Although behaviors of many specific moieties under oxygen delignification were patterned from these model studies, details about fragmentation or structural modification of the high molecular weight fraction of lignin, which are necessary for the technological development of oxygen delignification, are not yet clarified. One reason is the insufficient number of lignin model compounds with complicated and macromolecular architecture, but the main reason is probably the analytical difficulties presented by lignin itself. Therefore, many analytical methods, such as ^{31}P nuclear magnetic resonance (NMR) analysis, have been used after derivatization of lignin in order to analyze the structural modification of residual lignin during oxygen treatment.[4,5] However, the complexity of the task is not only due to the complex structures of lignin but also due to the complicated mechanisms of oxygen delignification.[6]

It is considered that delignification by oxygen is attributed to two different types of reaction. One is selective reaction toward lignin by molecular oxygen, and the other is the activity of other active oxygen species that are

generated during the oxygen treatment. As a matter of course, the active oxygen species contribute much to the removal or degradation of lignin, but these species lead also to the degradation of carbohydrate matrices of the pulp. As mentioned above, at least two types of reagents are included in the delignification mechanism. In such reaction systems with several reagents participating at the same time, it is difficult to observe the individual structural modifications that are brought about by each reagent. However, the generation and the decrease of each reagent should show certain temporal progress according to the kinetics of the respective reactions.

When the time course of oxygen treatment is monitored by spectroscopic methods or chemical degradation methods, the observed data should include temporal progress. In other words, observed data should be constituted as the product of the temporal progress and structural feature. In this case, the temporal progress should show the same trends by different measurement methods, although the structural features will be different because different analytical techniques reveal different chemical structures. Thus, if we can define temporal progress with certain functions, several sets of structural features can be identified by regression of the same set of temporal functions with observed spectra or determined values. The corresponding structural changes of lignin for each temporal feature can be discussed from different standpoints based on the nature of the analytical methods used.

As part of a fundamental study of the structural modifications to residual lignin in kraft pulp by the oxygen delignification process, time courses of some spectra or data obtained during alkaline oxygen treatment of kraft lignin were monitored in this study.

Materials and methods

Alkaline oxygen treatment

Five hundreds milliliters of aqueous solution containing 2.50 g of purified softwood kraft lignin and 10.0 g of sodium hydroxide (NaOH) was prepared. This solution was subjected to the alkaline oxygen treatment under 0.3 MPa oxygen pressure at 70°C. The specifications of the reactor are shown elsewhere. A small portion (about 25 ml) of the reaction mixture was withdrawn from the reactor at the various reaction periods. During the period in which the temperature was raised to 70°C, the reactor was pressurized to 0.3 MPa with nitrogen. The point of initial reaction (0 min) was defined as moment when, with the temperature at 70°C, the nitrogen in the reactor was completely displaced with oxygen. Same alkaline oxygen treatment was carried out twice with different withdrawing periods. The withdrawing periods for the first treatment were 0, 30, 90, 180, 380, and 1000 min. The periods for the second treatment were 0, 60, 120, 240, 600, and 1750 min.

Measurement of ultraviolet-visible spectra

The pH of 4 ml of each reaction mixture was adjusted to pH 8.5 with aqueous hydrochloric acid (HCl) and diluted to a volume of 50.0 ml with deionized water. Then 4.0 ml of this solution was diluted with a phosphate buffer solution (pH 11.5) to 50.0 ml and used for ultraviolet (UV)–visible measurement. UV-visible spectra were recorded in the range between 230 and 500 nm. Solution of phosphate buffer diluted with deionized water was used as the reference.

Preparation of neutralized reaction mixture for several measurements

Twenty milliliters of each reaction mixture was acidified to pH 4.0 with aqueous HCl solution, and then freeze-dried. The dried sample was dissolved in water, basified to pH 8.5 with aqueous NaOH, and diluted to a volume of 20.0 ml with a small amount of deionized water.

Infrared attenuated total reflectance spectroscopy

Infrared attenuated total reflectance (ATR) spectra of neutralized reaction mixtures were recorded using the method as already reported.[7]

Determination of total protons on unsaturated and aromatic system by ^{1}H-NMR spectra

Each 1.0-ml aliquot of neutralized reaction mixture was freeze-dried, and the residue dissolved in 0.5 ml deuterium oxide containing 1.0 mg/ml of 3-(trimethylsilyl)propionic-2,2,3,3-d_4 acid sodium salt (TSP-d_4) and 1% sodium deuteroxide (NaOD). ^{1}H-NMR spectra of these solutions were acquired, using TSP-d_4 as the internal standard for both quantification and chemical shift referencing. In order to flatten the spectrum baseline for the quantitative accuracy, a wide spectral width (25 000 Hz) was applied. The large H-O-D signal was depressed by selective irradiation. A straight baseline with intensities at –2.0 and 12.0 ppm of zero was set to each spectrum. From the ratio of peak area for 5.5–8.0 ppm and the TSP region (–0.04 to 0.04 ppm), total protons on the unsaturated and aromatic system was calculated.

Determination of ionization difference spectra and difference absorbance at 300 nm

A 0.30-ml aliquot of neutralized reaction mixture was diluted with 50 mM phosphate buffer to pH 11.5 and the volume was adjusted to 50 ml. Then the UV–visible spectrum under alkaline conditions was measured between 230 and 500 nm. A solution of phosphate buffer diluted with deionized water was used as the background.

Similarly, a 0.30-ml aliquot of neutralized reaction mixture was diluted with 50 mM acetate buffer to pH 5.5 and the volume was adjusted to 50 ml. Then the UV–visible spectrum was recorded under neutral conditions in the range between 230 and 500 nm. A solution of acetate buffer diluted with deionized water was used as the background. The difference spectrum for the spectra under alkaline and neutral conditions was calculated and the difference absorbance at 300 nm was determined.

Determination of methoxyl group content

A neutralized reaction mixture of 1.0 ml was freeze-dried. Determination of methoxyl group content was carried out for the dried mixture using the method as already reported.[8]

Results and discussion

Definition of the temporal progresses as functions by the analysis of the time course of UV-visible spectral change

Figure 1a shows the time course of UV-visible spectra of the reaction mixture during alkaline oxygen treatment of kraft lignin. Two different spectral changes, which appeared to have different temporal progresses, were clearly observed, as shown in Fig. 1a. They are a relatively fast increase at 350 nm (maximum at 120 min) and a subsequent slow decrease over the whole ultraviolet range respectively. In order to clarify the temporal progresses, which shows each spectral change, the number of spectral changes was investigated using singular value decomposition (SVD) of the whole set of UV-visible spectra. Appropriate functions for the temporal progresses were then sought.

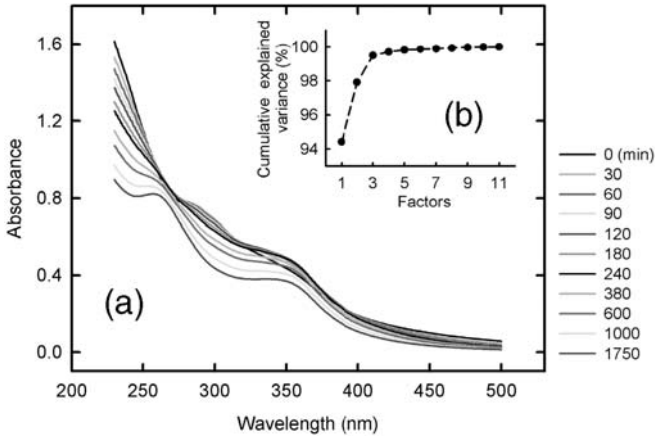

Fig. 1. **a** Time course of ultraviolet (UV)-visible spectra during alkaline oxygen treatment of kraft lignin, and **b** the cumulative explained variances calculated by singular value decomposition of the time course

The cumulative explained variance (Fig. 1b), which was obtained as a result of SVD, showed three primary factors accounted for 99.5% of spectral variance and other factors could be ignored. The decomposed factors obtained by SVD do not provide chemical information, but the number of factors should be the same as the number of actual spectral features. It was considered reasonable that the three spectral features include the pattern of an initial spectrum (predicted spectrum at 0 min), while the other two are the patterns of spectral changes from the initial spectrum. In this case, the corresponding three temporal progresses to each spectral feature could be defined as a constant and two temporal functions. If temporal progresses are described as such, the time courses of absorbance at each wavelength of the UV-visible spectra should be expressed as linear combinations of three temporal features.

Based on this consideration, the time course of UV-visible spectra was fitted with a linear combination of a constant and two temporal functions based on first-order or second-order decay. Following a fitting trial with three combinations, the combination of a constant and two temporal functions based on second-order decay [$F_1(t)$ and $F_2(t)$; half lives of 182 and 473 min, respectively] showed the best fitting result (Table 1). Spectral features [$A_{uv1}(\lambda)$, $A_{uv2}(\lambda)$, and $A_{uv3}(\lambda)$] corresponding to each temporal function were obtained (Fig. 2). In short, the time course of UV-visible spectra was decomposed as follows:

$$\left[\text{UV-vis absorbance at } \lambda \text{ nm}\right] = A_{uv1}(\lambda)F_1(t) + A_{uv2}(\lambda)F_2(t) + A_{uv3}(\lambda)$$

where

$$F_1(t) = 1 - 1/(1 + t/182), \quad F_2(t) = 1 - 1/(1 + t/473)$$

Temporal features represented by $F_1(t)$ and $F_2(t)$ are defined as "fast change" and "slow change," respectively. So the spectral feature $A_{uv1}(\lambda)$ shows the pattern of fast change, and $A_{uv2}(\lambda)$ shows the pattern of slow change. Because a positive band means an intensity increase with the progress of the treatment and negative means decreasing, $A_{uv1}(\lambda)$ indicates that the band intensity at 350 nm increases by fast change, and $A_{uv2}(\lambda)$ indicates that the decreasing

Table 1. Three linear combinations of temporal functions and evaluation of fitting results in the case of the time course of ultraviolet-visible spectra

Linear combinations	Optimized τ_1 (min)	Optimized τ_2 (min)	Error of sum of square
$a_1[1 - \exp(-t/\tau_1)] + a_2[1 - \exp(-t/\tau_2)] + a_3$	106	646	0.05
$a_1[1 - \exp(-t/\tau_1)] + a_2[1 - 1/(1 + t/\tau_2)] + a_3$	107	524	0.04
$a_1[1 - 1/(1 + t/\tau_1)] + a_2[1 - 1/(1 + t/\tau_2)] + a_3$	182	473	0.029

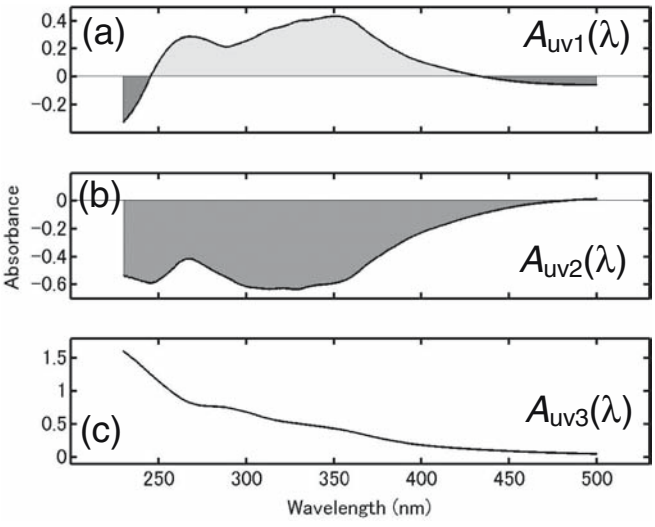

Fig. 2. Corresponding UV-visible spectral features for **a** "fast change," **b** "slow change," and **c** the initial spectrum. The spectra shown in **a–c** were obtained by the regression of temporal functions [$F_1(t) = 1 - 1/(1 + t/182)$, $F_2(t) = 1 - 1/(1 + t/473)$, and a constant] with the time course of UV-visible spectra. Positive intensity means increasing intensity with the progress of treatment; negative intensity means decreasing

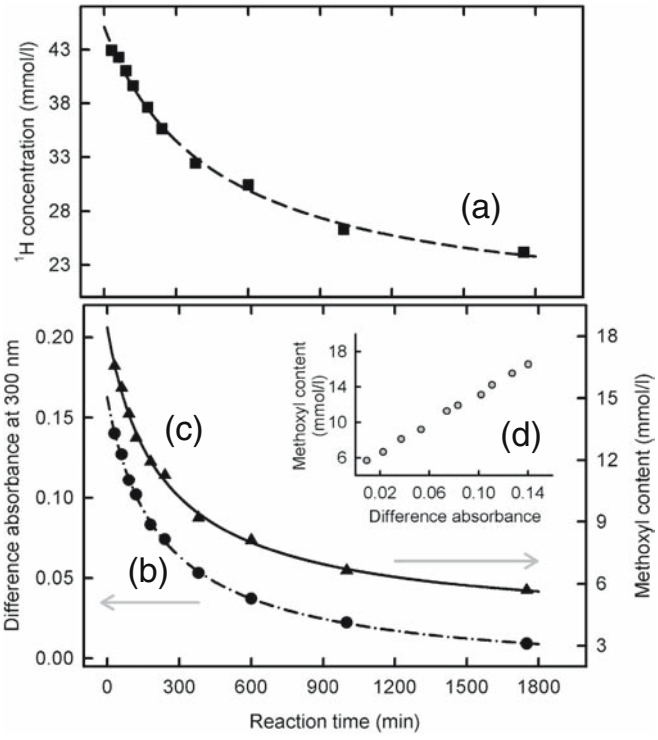

Fig. 3. The time courses of **a** total proton on the unsaturated and aromatic system, **b** ionization difference absorbance at 300 nm, and **c** methoxyl content. The approximated curves based on the temporal functions [$F_1(t) = 1 - 1/(1 + t/182)$, $F_2(t) = 1 - 1/(1 + t/473)$, and a constant] and their equations {**a**: $-26.8[0.035\ F_1(t) + 0.965\ F_2(t)] + 45.1$; **b**: $-0.175[0.771\ F_1(t) + 0.229\ F_2(t)] + 0.163$; **c**: $-14.6[0.753\ F_1(t) + 0.247\ F_2(t)] + 18.4$} are also described for each time course. **d** High correlation between difference absorbance at 300 nm and methoxyl content

intensity over the wide ultraviolet range occurs by slow change. These features properly represent the observed spectral changes over the time course of the UV-visible spectra.

Time course of total proton on unsaturated and aromatic system determined by ^{1}H-NMR

The temporal functions discussed above should fit not only the UV-visible spectra but also other spectral information from different analytical methods. The same temporal functions were fitted with the time course of the signals for total protons in the unsaturated and aromatic region of the NMR spectrum (Fig. 3a). The results showed a good fit, and the time course was approximated by a linear combination of temporal functions $F_1(t)$ and $F_2(t)$ as in the following equation:

$$\left[{}^1\text{H concentration}\,(\text{mM})\right] = -26.8\left[0.035\,F_1(t) + 0.965\,F_2(t)\right] + 45.1$$

This equation means that disappearance of total proton in the unsaturated and aromatic region by slow change is 96.5% in contrast with only 3.5% contribution of fast change. Very low contribution of fast change strongly indicates that the protons under scrutiny did not decrease by fast change. The chemical modification patterns occurring by fast change are thought to be the quantitative conversion of aromatic proton to unsaturated proton. The substructures resulting from fast change will be further degraded by slow change.

Time course of ionization difference absorbance at 300 nm

The time course of the ionization difference absorbance at 300 nm (Fig. 3b) was fitted to the temporal functions, which were defined from the analysis of UV-visible spectra, as in the case of total proton on the unsaturated and aromatic system. The fitting result showed that the time course of the difference absorbance was approximated well by a linear combination of temporal functions $F_1(t)$ and $F_2(t)$ as in the following equation:

$$\left[\text{Ionization difference absorbance at 300 nm}\right] = -0.175\left[0.771\,F_1(t) + 0.229\,F_2(t)\right] + 0.163$$

Because it is known that the ionization difference absorbance at 300 nm is proportional to the concentration of unconjugated phenolic substructure, this equation means that 77.1% of unconjugated phenolic substructure was degraded by fast change and another 22.9% was degraded by slow change. Although the contribution of fast change is relatively high, it was indicated that unconjugated phenolic substructure was degraded by both fast change and slow change. In addition, the high contribution of fast change could be explained by the high reactivity of unconjugated phenolic substructure toward alkaline oxygen treatment.

Time course of methoxyl content

Figure 3c shows the time course of methoxyl content during the alkaline oxygen treatment of kraft lignin. This time course also showed good fitting when the temporal functions were used, and was approximated by the following equation:

$$\left[\text{Methoxyl content (mM)}\right] = -14.6\left[0.753\,F_1(t) + 0.247\,F_2(t)\right] + 18.4$$

This equation revealed that 75.3% of the decrease of methoxyl content is attributed to fast change and another 24.7% to slow change. Although the contribution of fast change is relatively high, it was revealed that methoxyl group was eliminated by both fast and slow change. When the time course of methoxyl content was compared with that of ionization difference absorbance at 300 nm, as shown in Fig. 3d, two determined values are correlated positively with a very high correlation coefficient (R = 0.9993). This correlation could indicate that the degradation of unconjugated phenolic substructure and the elimination of methoxyl group occurred at the same time by both fast and slow change.

By integrating these considerations and the results from the time course of total protons on the unsaturated and aromatic system, possible major reactions that occurred by fast change could be suggested. One is formation of muconate derivative from the phenolic substructure through a ring-opening reaction, and another is the generation of an *ortho*-quinone substructure from the phenolic substructure (Fig. 4). Both reactions do not alter the total number of protons on the unsaturated and aromatic system, and lead to the elimination of methoxyl group as a result of the decrease of phenolic substructure.

Time course of the infrared ATR spectra

Figure 5 shows the time course of infrared ATR spectra during alkaline oxygen treatment. It is obvious that an increase of carboxlate group (asymmetric stretching: 1570 cm^{-1}, symmetric stretching: 1380 cm^{-1}), particularly oxalate (1310 cm^{-1}), and a decrease of the bond between aromatic carbon and oxygen (C_{arom}–O: 1220 and 1270 cm^{-1}) and the bond between aromatic carbon and hydrogen (C_{arom}–H: 1030 and 1130 cm^{-1}) occurred with the progress of the treatment.

Temporal functions were again fitted well with the time course of infrared ATR spectra, and the corresponding spectral features [$A_{IR1}(\nu)$, $A_{IR2}(\nu)$, and $A_{IR3}(\nu)$] were obtained (Fig. 6). In short, the time course of infrared ATR spectra was decomposed as follows:

$$\left[\text{Infrared ATR absorbance at } \nu\ \text{cm}^{-1}\right] = A_{IR1}(\nu)\cdot F_1(t) + A_{IR2}(\nu)\cdot F_2(t) + A_{IR3}(\nu)$$

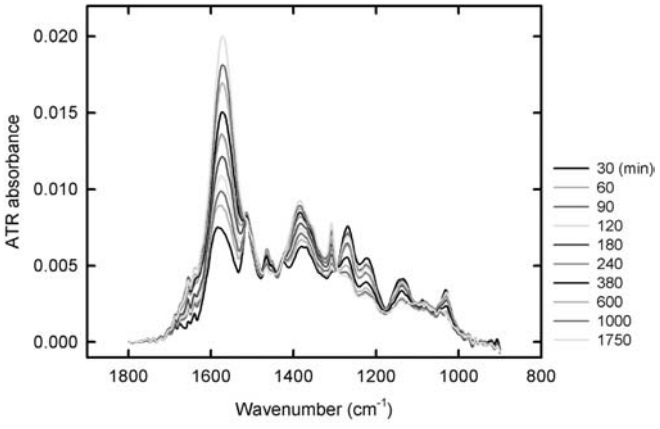

Fig. 5. Time course of infrared attenuated total reflectance (ATR) spectra during alkaline oxygen treatment of kraft lignin

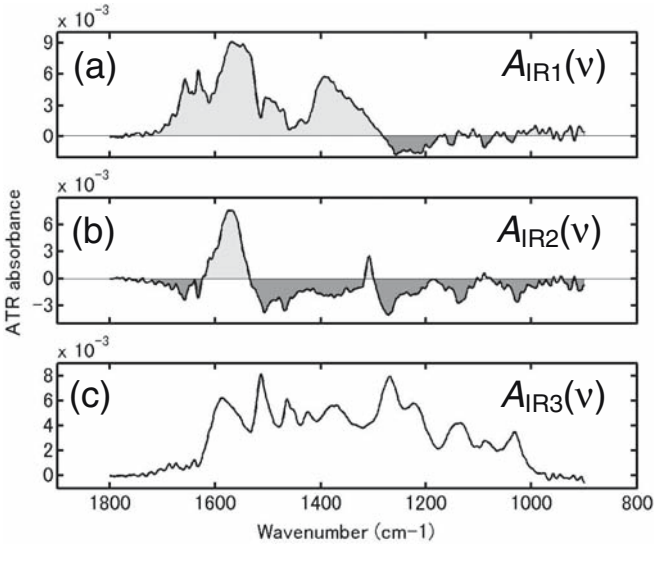

Fig. 6. Corresponding infrared ATR spectral features for **a** fast change, **b** slow change, and **c** the initial spectrum. The spectra shown in **a–c** were obtained by regression of temporal functions [$F_1(t) = 1 - 1/(1 + t/182)$, $F_2(t) = 1 - 1/(1 + t/473)$, and a constant] with the time course of infrared ATR spectra

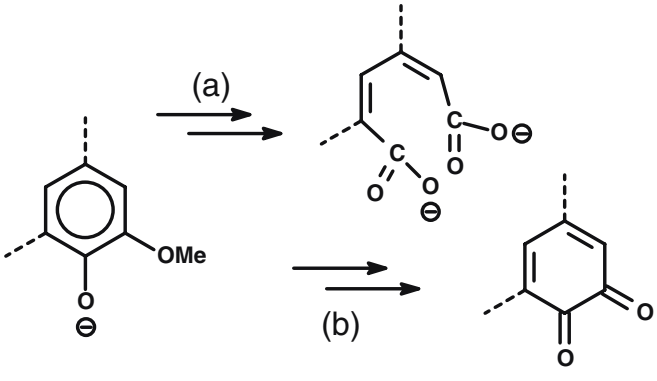

Fig. 4a,b. Two possible major chemical modifications of kraft lignin by fast change of alkaline oxygen treatment. **a** Generation of muconate derivative; **b** generation of *ortho*-quinone substructure

The spectral feature $A_{IR1}(\nu)$ shows the pattern of spectral change by fast change, and $A_{IR2}(\nu)$ shows slow change as in the case of UV-visible spectra. $A_{IR3}(\nu)$ shows the pattern of the initial spectrum. The spectral feature of fast change, $A_{IR1}(\nu)$, indicates that carboxylate was generated and C_{arom}–O bond was degraded by fast change. Decrease of the aromatic skeleton by fast change was not observed as a negative band but only a valley (particularly 1510 cm^{-1}) was found probably because of the strong intensity of carboxylate bands.

These spectral data of fast change strongly support that the reaction, by which a phenolate substructure changes into a muconate derivative through a ring-opening reaction, is one of the major reactions occurring by fast change. The generation of muconate derivatives leads to the quantitative conversion of aromatic proton to unsaturated proton, elimination of methoxyl group and generation of carboxylate. Of course, it does not mean that the reactions of generating *ortho*-quinone substructure do not occur by fast change.

The spectral feature of slow change, $A_{IR2}(\nu)$, showed the decrease of the aromatic structure of lignin (C_{arom}–H, C_{arom}–O, methoxyl group, and aromatic skeletal vibration), and the increase of oxalate. There is no doubt that further degradation of aromatic structure of lignin occurred by slow change.

pH dependence of UV absorbance at 350 nm

The reactions of fast change are not constituted only by the generation of muconate derivative. In fact, when the time course of UV-visible spectra was decomposed, the spectral feature of fast change clearly showed the increase of the band at around 350 nm (Fig. 2). This phenomenon, although it is specific for fast change, cannot be explained by the generation of muconate derivatives.

Figure 7 shows the UV-visible spectral changes when the measurement pH was changed. In this figure, the absorbance readings at 350 nm were differentiated with respect to the measurement pH so that the pH at top peak on this figure should be the pK_a. Because the band intensity changes with pH, the chemical structure corresponding to the absorbance at around 350 nm under alkaline conditions is thought to be a phenolate substructure and its pK_a is estimated to be around 8.0. Furthermore, it is important to note that the phenolate substructure of this type shows high resistance toward alkaline oxygen treatment because the band still remains after a very long treatment time (5780 min).

This means that some phenolic substructures that are resistant toward alkaline oxygen treatment are generated by fast change, and the degradation of these substructures is difficult by slow change and fast change. Some α-carbonyl-type phenolic substructures might be the possible candidate for such substructures because of their lower pK_a values and inertness toward alkaline oxygen treatment.

Because the muconate derivatives are thought to be generated by the reaction of molecular oxygen and subsequently generated superoxide anion radical with the phenolic substructure according to the studies of lignin model compounds, the defined fast change may well represent the chemical modifications by molecular oxygen and superxide anion radical. Therefore, the resistant α-carbonyl-type phenolic substructure may also be generated by the reactions of these oxygen species with some specific substructure in kraft lignin.

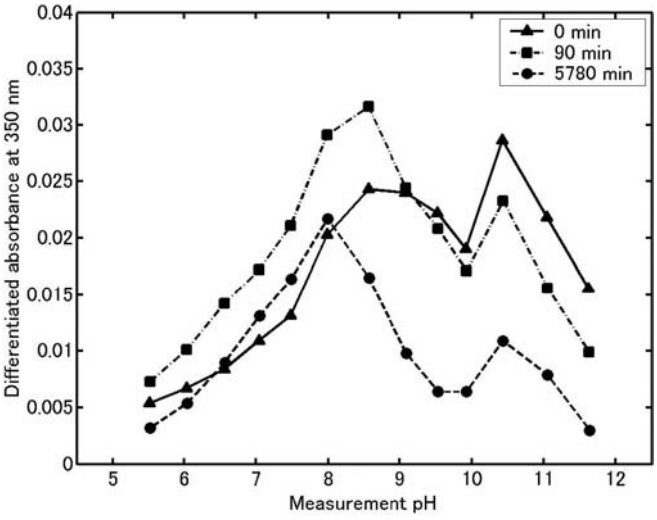

Fig. 7. UV-visible spectral changes of reaction mixture when measurement pH was changed. The absorbance values at 350 nm were differentiated with respect to pHs

The *ortho*- and *para*-stilbene substructures, which are generated from the phenylcoumaran unit in native lignin during kraft cooking, may be one candidate of such a substructure.[9] From this structure, the corresponding α-carbonyl-type phenolic substructures ought to be generated through the reaction with molecular oxygen and superoxide anion radical. However, many other possible mechanisms or origins for the resistant α-carbonyl-type phenolic substructure, for example, the oxidation of unconjugated phenolic substructure with benzylic hydroxyl groups, could still exist.

Conclusions

For the fundamental study of lignin degradation during oxygen delignification, the progress of degradation of kraft lignin during alkaline oxygen treatment was monitored using several spectroscopic or chemical degradation techniques. Two temporal processes inherent in the treatment (fast change and slow change) were defined as two different functions, and the corresponding spectral features or contributions of each temporal process were calculated. By integrating this information about structural changes, the major reactions occurring during each temporal process were suggested. The generation of muconate derivatives from unconjugated phenolic substructure was strongly indicated as one of major reactions occurring by fast change in the

alkaline oxygen treatment of kraft lignin. Although the generation of muconate derivative is favorable for the efficiency of oxygen delignification because this reaction makes the lignin more soluble, the generation of a resistant α-carbonyl-type phenolic substructure was suggested was also suggested as a major chemical modification occurring by fast change. Because this substructure is one of most resistant moieties in oxygen delignification, further investigation about the mechanisms of the generation of α-carbonyl-type phenolic substructures will be important for the technological development of oxygen delignification and subsequent bleaching process.

References

1. Olm L, Teder A (1979) The kinetics of oxygen bleaching. TAPPI 62:43–46
2. Ljunggren S, Johansson E (1990) The kinetics of lignin reactions during oxygen bleaching part 3. Holzforschung 44:291–296
3. Johansson E, Ljunggren S (1994) The kinetics of lignin reactions during oxygen bleaching part 4. J Wood Chem Technol 14:507–525
4. Gellerstedt G, Gustafsson K, Lindfors EL (1986) Structural changes in lignin during oxygen bleaching. Nord Pulp Paper Res J 1:14–17
5. Akim LG, Colodette JL, Argyropoulos DS (2001) Factors limiting oxygen delignification of kraft pulp. Can J Chem 79:201–210
6. Gierer J, Reitberger T, Yang E, Yoon BH (2001) Formation and involvement of radicals in oxygen delignification studied by the autooxidation of lignin and carbohydrate model compounds. J Wood Chem Technol 21:313–341
7. Yada M, Shintani H, Meshitsuka G (2005) Infrared spectroscopic study of alkaline oxygen treatment of lignin with ATR technique in aqueous state 1. J Wood Sci 51:239–245
8. Goto H, Koda K, Tong G, Matsumoto Y, Meshitsuka G (2005) Formation of methyl iodide from methoxyl-free compounds by hydriodic acid treatment. J Wood Sci 51:312–314
9. Adler E, Marton J, Falkehag I (1964) The behavior of lignin in alkaline pulping 1. Model experiments with phenylcoumarans. Acta Chem Scand 18:1311–1312